Available online at www.sciencedirect.com

ScienceDirect

Ceramics International 40 (2014) 605–609

CERAMICS INTERNATIONAL

www.elsevier.com/locate/ceramint

Preparation of (100) CeO_2 and (110) $YBa_2Cu_3O_{7-\delta}$ films by laser chemical vapor deposition

Pei Zhao, Akihiko Ito*, Takashi Goto

Institute for Materials Research, Tohoku University, 2-1-1 Katahira, Aoba-ku, Sendai 980-8577, Japan

Received 14 May 2013; received in revised form 11 June 2013; accepted 12 June 2013
Available online 19 June 2013

Abstract

CeO_2 and $YBa_2Cu_3O_{7-\delta}$ (YBCO) films were prepared by laser chemical vapor deposition. The (100)-oriented CeO_2 films prepared at 975–1088 K consisted of columnar grains with pyramidal caps of the CeO_2 {111} planes. The deposition rate was 3.0–5.4 μm h^{-1}. The (110)-oriented YBCO films were prepared on the (100)-oriented CeO_2 films at a deposition temperature of 1004 K. The (110)-oriented YBCO films showed wedge-shaped grains.

Keywords: A. Film; D. CeO_2; Laser CVD; YBCO; Orientation control

1. Introduction

The high-temperature superconductor $YBa_2Cu_3O_{7-\delta}$ (YBCO) has been extensively studied since its discovery in 1987 [1,2]. The electrical transport properties of YBCO are highly anisotropic and depend greatly on the crystallographic orientation [3,4]. Since YBCO can carry a large superconducting current along the CuO_2 plane (*ab*-plane), *c*-axis-oriented YBCO films are required for high-temperature superconducting power cables. YBCO also exhibits a photovoltaic effect [5]. Because the coherence length along the *ab*-plane (ξ_{ab}=1.2–15 nm) is much larger than that along the *c*-axis (ξ_c=0.1–0.3 nm) [6,7], (110)-oriented YBCO films are preferable in photovoltaic devices [8].

(110)-oriented YBCO films have been prepared on the (110) planes of single crystal substrates, mainly $SrTiO_3$ [9–12]. However, (103)-oriented YBCO was often observed with (110)-oriented grains because of the alternating coherent epitaxial relationship between the YBCO (103) plane and substrate. We previously prepared (100)-oriented CeO_2 films on single crystal and polycrystalline substrates by laser chemical vapor deposition (laser CVD) [13,14]. The CeO_2 films consisted of columnar grains and showed strong (100) orientation. The top of the (100)-oriented CeO_2 columnar grain was terminated by pyramidal caps of the CeO_2 {111} plane. In these studies, a metalorganic (MO) compound of Ce was used as a solid precursor. Although MOCVD process using a solid compound has widely been studied, in terms of preparing multi-component film in industrial applications, a stable and continuous precursor feeding system using a single liquid precursor is feasible for a long-length production of CeO_2 and YBCO films.

In the present study, by utilizing the pyramidal morphology of CeO_2 film as a template, (110)-oriented YBCO films were prepared on (100)-oriented CeO_2 films.

2. Experimental

The laser CVD apparatus used in this study is depicted in Fig. 1. A continuous wave Nd:YAG laser (wavelength: 1064 nm) was employed. CeO_2 films were prepared using $Ce(DPM)_4$ (dipivaloylmethanate; DPM) dissolved in C_4H_8O (tetrahydrofuran; THF) at a concentration of 0.116 mol L^{-1}. The source solution was delivered at a supply rate of 0.25×10^{-4} L s^{-1} by a plunger pump. The flow rates of Ar and O_2 gases were 1.52 and 0.34 Pa m^3 s^{-1}, respectively. The evaporation chamber was heated to 653 K. A multilayer-coated Hastelloy C276 tape

*Corresponding author. Tel.: +81 22 215 2106; fax: +81 22 215 2107.
E-mail address: itonium@imr.tohoku.ac.jp (A. Ito).

0272-8842/$ - see front matter © 2013 Elsevier Ltd and Techna Group S.r.l. All rights reserved.
http://dx.doi.org/10.1016/j.ceramint.2013.06.041

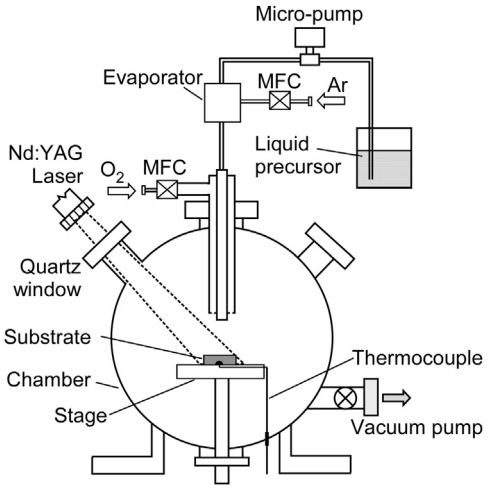

Fig. 1. A schematic of laser CVD apparatus using a single liquid source precursor delivery system.

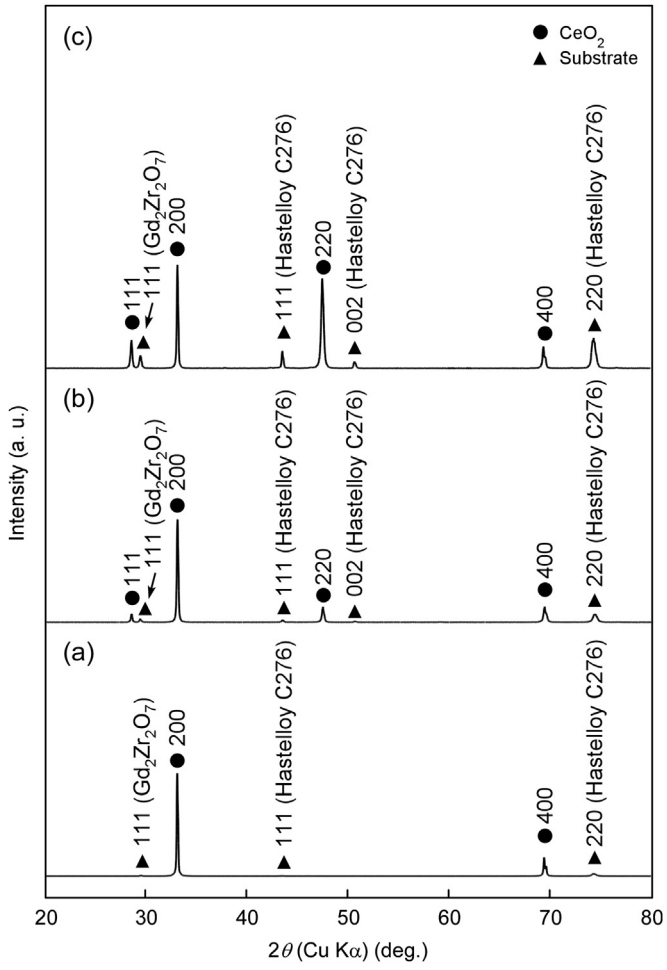

Fig. 2. XRD patterns of CeO_2 films prepared at T_{dep} = 1040 K (a), 1110 K (b) and 1134 K (c).

(10 mm × 5 mm × 0.1 mm) with a structure of $LaMnO_3$/MgO/$Gd_2Zr_2O_7$/Hastelloy C276 was used as a substrate and was preheated on a hot stage at 823 K. The total pressure was maintained at 0.8 kPa.

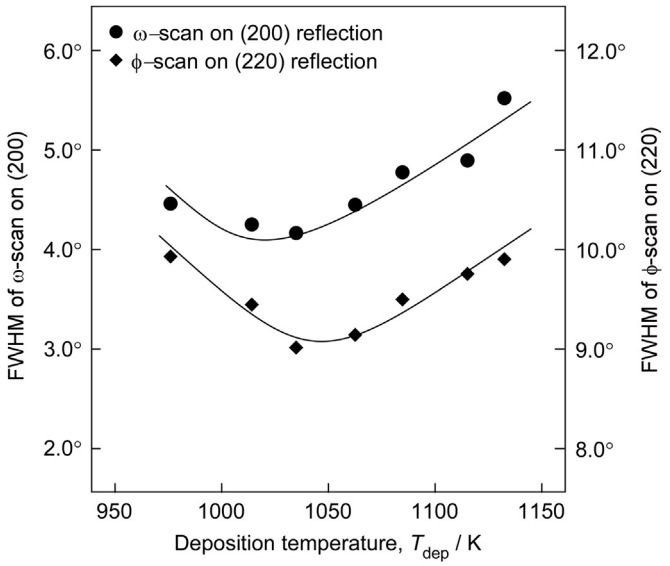

Fig. 3. Effect of T_{dep} on the FWHM of ω-scan on the (200) reflection and that of ϕ-scan on the (220) reflection of the CeO_2 films.

YBCO films were prepared using $Y(DPM)_3$, $Ba(DPM)_2$/$Ba(TMOD)_2$ (2,2,6,6-tetramethyl-3,5-octanedionate; TMOD) and $Cu(DPM)_2$. These were mixed in a molar ratio of Y:Ba:Cu = 1:2.4:2.8 and then dissolved in THF in a concentration of 0.01 mol L^{-1} of Y. The source solution was delivered at a supply rate of 0.11×10^{-4} L s^{-1}. The substrate preheating temperature was 923 K. The flow rate of O_2 gas was 0.85 Pa m^3 s^{-1}.

The phases and orientations of the CeO_2 and YBCO films were identified using an X-ray diffractometer (XRD; Rigaku RAD-2C). The crystallinity of the CeO_2 film was evaluated from the full width at half maximum (FWHM) of the ω-scan (rocking curve) of the (200) reflection. The in-plane orientation of the CeO_2 film was evaluated from the FWHM of the ϕ-scan of the (220) reflection, which was measured by a pole figure XRD (Rigaku Ultima IV). The microstructure was observed using a field emission scanning electron microscope (FESEM; JEOL JSM-7500F). A schematic of the crystal structure was drawn using VESTA [15].

3. Results and discussion

The deposition temperature (T_{dep}) increased from 975 to 1134 K with laser power (P_L) from 46 to 132 W. Fig. 2 shows the XRD patterns of the CeO_2 films prepared at T_{dep} = 975–1134 K. (100)-oriented CeO_2 films were obtained at T_{dep} = 975–1088 K (Fig. 2(a)). Small peaks of (111) and (220) orientations were observed in the diffraction patterns of the (100)-oriented CeO_2 films at T_{dep} = 1110–1134 K (Fig. 2(b)).

Fig. 3 shows the effect of T_{dep} on the FWHM values of the ω-scan of the (200) reflection and that of the ϕ-scan of the (220) reflection of the CeO_2 films. With increasing T_{dep} from 975 to 1134 K, the FWHM values of the ω-scan first decreased from 4.3° to 4.1° and then increased to 5.4°, with a minimum of 4.1° at T_{dep} = 1040 K. The FWHM values of the ϕ-scan of the (220) reflection of the CeO_2 films first decreased from 9.9°

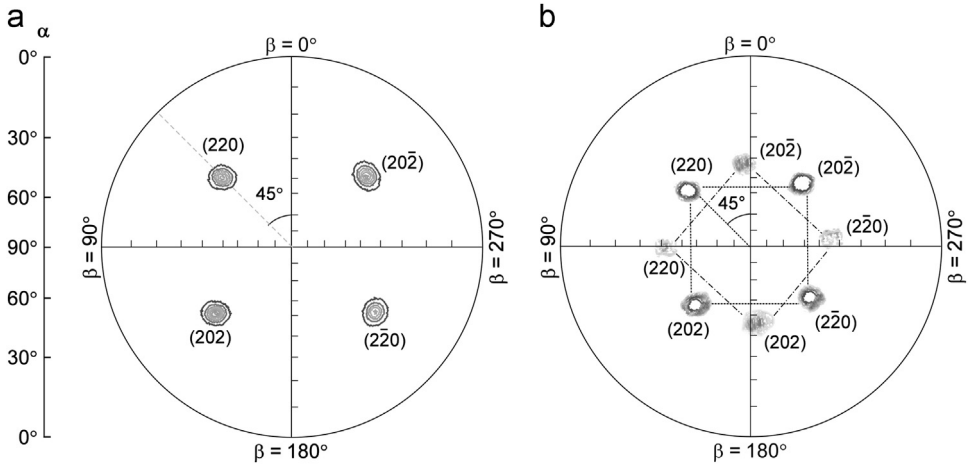

Fig. 4. X-ray pole figure patterns of the (220) reflection of the CeO_2 films prepared at T_{dep} = 1040 K (a) and 1110 K (b).

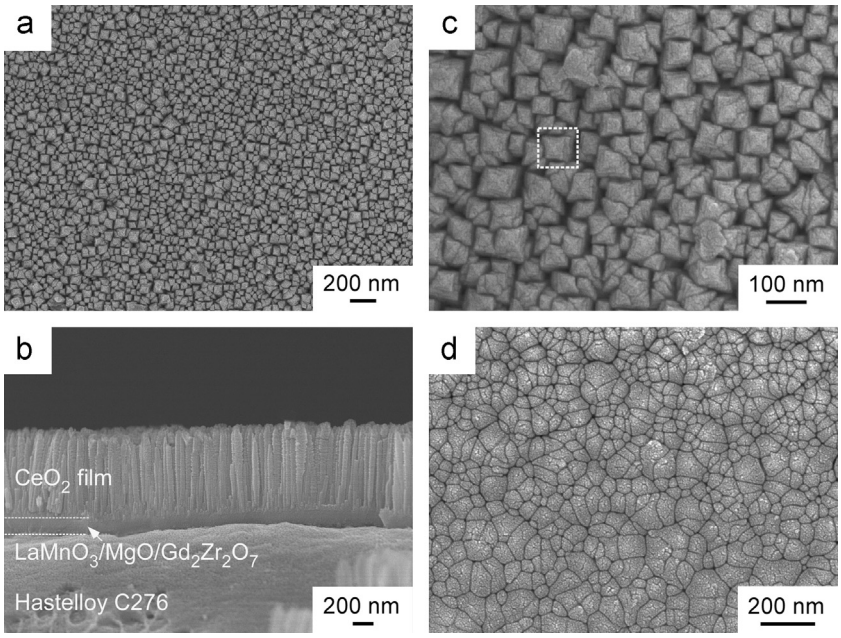

Fig. 5. FESEM images of CeO_2 films prepared at T_{dep} = 1040 K (a)–(c) and 1134 K (d).

to 9.0° and then increased to 9.8°, with a minimum of 9.0° at T_{dep} = 1040 K. For the CeO_2 films prepared on multilayer-coated Hastelloy C273 tape by laser CVD using a solid precursor, the FWHM values of ω- and ϕ-scan were 4.3° and 6.0°, respectively [14]. Thus, the present CeO_2 films prepared using a liquid precursor were comparable to the CeO_2 films prepared using a solid precursor.

Fig. 4 shows the XRD pole figures of the (220) reflection of the CeO_2 films prepared at T_{dep} = 1040 and 1110 K. The pole figure of the (220) reflection of the CeO_2 films prepared at T_{dep} = 975–1088 K showed a fourfold pattern at approximately α = 45° (Fig. 4(a)). This was attributed to the (220) plane with the complementary angle of 45° to the (100) plane. For the CeO_2 films prepared at T_{dep} = 1110 K (Fig. 4(b)), the pole figures showed two groups of diffraction patterns, which consisted of strong fourfold reflections and weak fourfold reflections. These diffraction patterns were attributed to the (220) plane with the complementary angle of 45° to the (100) plane. The azimuth angle β of 45° between strong and weak reflections indicates a 45° rotation for a small volume faction of (100)-oriented grains. In the case of the CeO_2 film prepared at T_{dep} = 1134 K, no poles were observed in the diffraction patterns of the (220) reflection because of the dominance of the (111)-oriented grains in the CeO_2 film (Fig. 2(c)).

Fig. 5 shows the microstructures of the CeO_2 films prepared at T_{dep} = 1040 and 1134 K. The low magnification image of the CeO_2 film prepared at T_{dep} = 1040 K shows pyramidal surface grains (Fig. 5(a)). The cross-sectional image shows a columnar growth of the CeO_2 film (Fig. 5(b)). The magnified surface image of the fine grains prepared at T_{dep} = 1100 K (Fig. 5(c)) shows orthogonal pyramidal caps whose four-sided facets were attributed to the {111} planes [16]. Because the {111} planes have the lowest surface energy compared to the (100) and (110) planes [17,18], they would be preferentially formed at

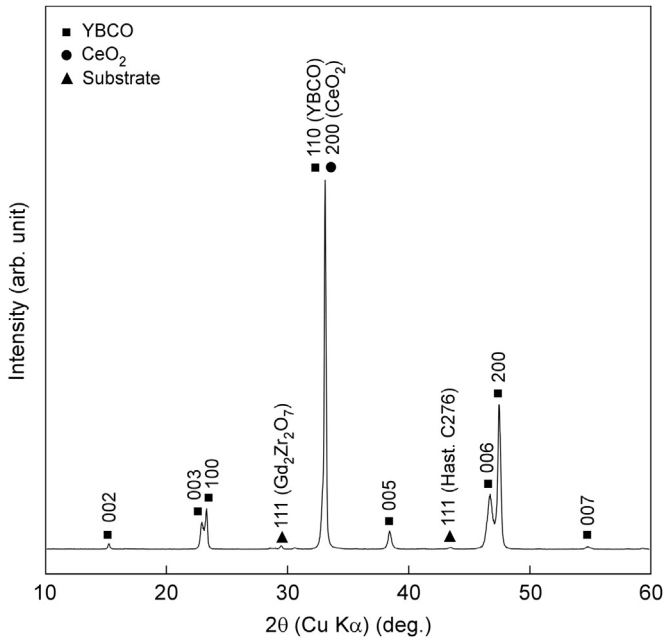

Fig. 6. XRD pattern of the YBCO films prepared at T_{dep} = 1016 K on CeO_2 film.

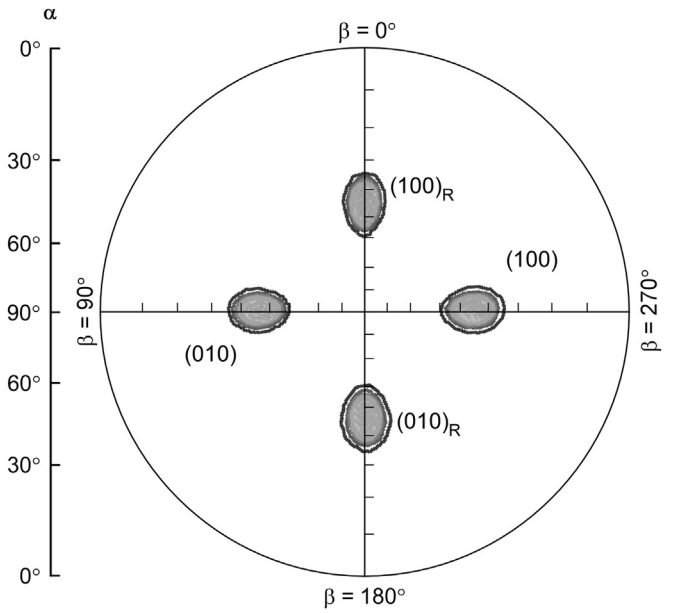

Fig. 7. X-ray pole figure pattern of the YBCO films prepared at T_{dep} = 1016 K on CeO_2 film.

the top surface of the CeO_2 film. The size of columnar grains was approximately 50 nm in width and was finer than the columnar grains obtained in the CeO_2 films prepared using a solid precursor (approximately 80 nm in width) [14]. The CeO_2 film prepared at T_{dep} = 1134 K consisted of granular grains (Fig. 5(d)). The deposition rate (R_{dep}) of the CeO_2 film prepared was 4.8–5.4 μm h^{-1} at T_{dep} = 975–1040 K. A further increase in T_{dep} to 1134 K caused a decrease of R_{dep} to 3.6 μm h^{-1}. The R_{dep} of the CeO_2 films prepared using a liquid precursor was slightly higher than those of films prepared using a solid precursor (3.4–4.6 μm h^{-1}) [14]. The optimized T_{dep} for the (100)-oriented CeO_2 film was 1040 K (the corresponding P_L was 77 W), at which the CeO_2 film showed the highest in-plane orientation (Fig. 3).

The YBCO films were prepared at T_{dep} = 1004 K (P_L = 85 W) on the (100)-oriented CeO_2 films. Fig. 6 shows the XRD pattern of the YBCO film, which showed a (110) preferred orientation. The XRD peak of the YBCO (110) plane (2θ = 32.8°) overlapped with that of the CeO_2 (200) plane (2θ = 33.1°). A small amount of YBCO grains with *a*-axis and *c*-axis orientations was also present in the (110)-oriented YBCO film.

Fig. 7 shows the X-ray pole figure of the (100) reflection of the (110)-oriented YBCO film prepared at T_{dep} = 1004 K on (100)-oriented CeO_2 film. The YBCO (100) reflection showed four spots at approximately α = 45°. This was attributed to the YBCO (100) plane with the complementary angle of 45° to the YBCO (110) plane. Because the YBCO (100) plane exhibits twofold reflections for YBCO (110) plane, the fourfold reflections observed in the pole figure suggested that (110)-oriented YBCO grains had a 90°-rotated domain (indicated as R in Fig. 7). The in-plane orientation relationship between (110)-oriented YBCO and (100)-oriented CeO_2 films was [001] YBCO∥[011] CeO_2.

Fig. 8 shows the surface and cross-sectional FESEM images of the YBCO film prepared at T_{dep} = 1004 K on (100)-oriented CeO_2 film. The low magnification surface image of the (110)-oriented YBCO film shows a dense surface with crystal grains approximately 200–300 nm in size (Fig. 8(a)). The magnified surface image shows that the (110)-oriented YBCO film consists of crystal grains with wedge-shaped top surfaces. The four facets of these wedge-shaped grains could be the {100} and {001} planes. R_{dep} of the (110)-oriented YBCO film was 8.7 μm h^{-1}. Image (d) depicts the growth relationship between (110)-oriented YBCO grains and the (100)-oriented CeO_2 grains with pyramidal caps of the {111} planes. Between two neighboring CeO_2 grains, a V-shaped valley can be formed along the ⟨110⟩ direction, as shown in Fig. 8(d). At the nucleation stage of the YBCO film, the V-shaped valley could serve as the knit sites for the (110)-oriented YBCO grains to decrease the total surface energy while the YBCO nucleates at these sites [19]. Therefore, (110)-oriented YBCO grains could favorably grow on the (100)-oriented CeO_2 grains. These wedge-shaped grains were perpendicular to each other, as marked in Fig. 8. This grain growth model is coincident with the in-plane orientations derived from the X-ray pole figure analysis (Figs. 4 and 6).

4. Conclusions

CeO_2 films with (100) preferred orientation were prepared at a high deposition rate of 3.0–5.4 μm h^{-1} on multilayer-coated Hastelloy C276 tape by laser CVD. The FWHM of the ω-scan of the (200) reflection and that of the ϕ-scan of the (220) reflection were 4.1–5.4° and 9.0–9.9°, respectively. The (100)-oriented CeO_2 films had columnar grains in the cross section. The YBCO film with (110) preferred orientation was prepared on (100)-oriented CeO_2 films at a high

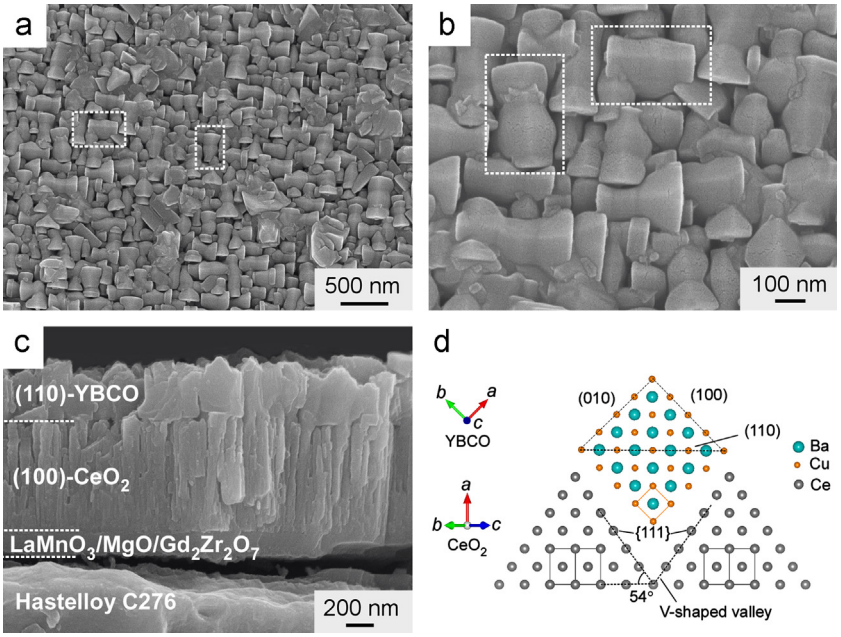

Fig. 8. FESEM surface (a) and cross-sectional (c) images of the (110)-oriented YBCO film prepared at T_{dep} = 1004 K. Image (b) is the magnified surface image. Image (d) depicts the growth relationship between the (110)-oriented YBCO grains and the (100)-oriented CeO_2 grains.

deposition rate of 8.7 μm h^{-1}. The (110)-oriented YBCO film showed wedge-shaped grains.

Acknowledgments

This work was supported in part by the International Superconductivity Technology Center (ISTEC). This work was also supported in part by the Japan Society for the Promotion of Science, Grant-in-Aid for Young Scientists (A) (25709069) and Challenging Exploratory Research (25630273), and the 111 Project, China (B13035).

References

[1] K.A. Müller, J.G. Bednorz, The discovery of a class of high-temperature superconductors, Science 237 (1987) 1133–1139.
[2] M.K. Wu, J.R. Ashburn, C.J. Torng, P.H. Hor, R.L. Meng, L. Gao, et al., Superconductivity at 93 K in a new mixed-phase Y-Ba-Cu-O compound system at ambient pressure, Physical Review Letters 58 (1987) 908–910.
[3] T.R. Dinger, T.K. Worthington, W.J. Gallagher, R.L. Sandstrom, Direct observation of electronic anisotropy in single-crystal $Y_1Ba_2Cu_3O_{7-x}$, Physical Review Letters 58 (1987) 2687–2690.
[4] S.W. Tozer, A.W. Kleinsasser, T. Penney, D. Kaiser, F. Holtzberg, Measurement of anisotropic resistivity and Hall constant for single-crystal $YBa_2Cu_3O_{7-x}$, Physical Review Letters 59 (1987) 1768–1771.
[5] C.L. Chang, A. Kleinhammes, W.G. Moulton, L.R. Testardi, Symmetry-forbidden laser-induced voltages in $YBa_2Cu_3O_7$, Physical Review B 41 (1990) 11564–11567.
[6] R.B. Laibowitz, R.H. Koch, A. Gupta, G. Koren, W.J. Gallagher, V. Foglietti, et al., All high Tc edge junctions and SQUIDs, Applied Physics Letters 56 (1990) 686–688.
[7] H.-U. Habermeier, A.A.C.S. Lourenço, B. Friedl, J. Kircher, J. Köhler, The growth of (110) Y-Ba-Cu-O thin films and their characterization by optical methods, Solid State Communications 77 (1991) 683–687.
[8] H.S. Kwok, J.P. Zheng, S.Y. Dong, Origin of the anomalous photovoltaic signal in Y–Ba–Cu–O, Physical Review B 43 (1991) 6270–6272.
[9] S. Poelders, R. Auer, G. Linker, R. Smithey, R. Schneider, Transition from (110) to (103)/(013) growth in $Y_1Ba_2Cu_3O_{7-x}$ thin films on (110) $SrTiO_3$ substrates, Physica C 247 (1995) 309–318.
[10] G. Linker, X.X. Xi, O. Meyer, Q. Li, J. Geerk, Control of growth direction of epitaxial YBaCuO thin films on $SrTiO_3$-substrates, Solid State Communications 69 (1989) 249–253.
[11] A.L. Vasiliev, D.S. Linehan, E.P. Kvam, L. Hou, M.W. McElfresh, Single variant orientational growth of $YBa_2Cu_3O_{7-x}$ on vicinal (011) $SrTiO_3$ substrates observed by electron microscopy, Physica C 289 (1997) 243–250.
[12] M. Guilloux-Viry, C. Thivet, A. Perrin, M. Sergent, M.G. Karkut, C. Rossel, et al., Crystal growth of (110) and (103) $YBa_2Cu_3O_7$ thin films in-situ deposited by laser ablation on (110) $SrTiO_3$ single-crystal substrates, Journal of Crystal Growth 132 (1993) 396–404.
[13] P. Zhao, A. Ito, R. Tu, T. Goto, High-speed epitaxial growth of (100)-oriented CeO_2 film on r-cut sapphire by laser chemical vapor deposition, Surface and Coatings Technology 205 (2011) 4079–4082.
[14] P. Zhao, A. Ito, R. Tu, T. Goto, Influence of laser power on the orientation and microstructure of CeO_2 films deposited on Hastelloy C276 tapes by laser chemical vapor deposition, Applied Surface Science 256 (2010) 6395–6398.
[15] K. Momma, F. Izumi, VESTA 3 for three-dimensional visualization of crystal, volumetric and morphology data, Journal of Applied Crystallography 44 (2011) 1272–1276.
[16] S.N. Jacobsen, U. Helmersson, R. Erlandsson, B. Skårman, L.R. Wallenberg, Sharp microfaceting of (001)-oriented cerium dioxide thin films and the effect of annealing on surface morphology, Surface Science 429 (1999) 22–33.
[17] T.X.T. Sayle, S.C. Parker, C.R.A. Catlow, The role of oxygen vacancies on ceria surfaces in the oxidation of carbon monoxide, Surface Science 316 (1994) 329–336.
[18] J. Conesa, Computer modeling of surfaces and defects on cerium dioxide, Surface Science 339 (1995) 337–352.
[19] J.A. Venables, Introduction to Surface and Thin Film Processes, 1st ed., Cambridge University Press, Cambridge, UK, 2000.